Available online at www.sciencedirect.com
SCIENCE DIRECT
International Journal of Heat and Mass Transfer 49 (2006) 1493–1500
International Journal of HEAT and MASS TRANSFER
www.elsevier.com/locate/ijhmt

A numerical study on ultra-short pulse laser-induced damage on dielectrics using the Fokker–Planck equation

Young Min Oh [a], Seong Hyuk Lee [b], Seungho Park [c], Joon Sik Lee [a,*]

[a] *School of Mechanical and Aerospace Engineering, Seoul National University, Seoul 151-742, Republic of Korea*
[b] *School of Mechanical Engineering, Chung-Ang University, Seoul 156-756, Republic of Korea*
[c] *Department of Mechanical and System Design Engineering, Hongik University, Seoul 121-791, Republic of Korea*

Received 5 June 2003; received in revised form 15 July 2005
Available online 6 December 2005

Abstract

Extensive numerical simulations are conducted to investigate the characteristics of ultra-short pulse laser-induced breakdowns of fused silica at different wavelengths of 526, 780, and 1053 nm. The Fokker–Planck (F–P) equation is applied to describe the transient behaviors of electron densities and to predict the damage threshold fluences for various laser pulse widths ranging from 10 fs to 10 ps, including the effects of electron avalanche and multiphoton ionization (MPI) on the generation of electrons. The predicted damage threshold fluences are in good agreements with experimental observations. The damage threshold fluences increase with laser pulse durations and laser wavelengths, and for longer pulses the impact ionization becomes more effective in increasing the electron number density than the MPI. In addition, the damage fluences have been calculated when both alternating current electric fields and ultra-short pulse lasers are simultaneously applied to the dielectric materials. As the electric field intensities increase, the damage threshold fluences decrease considerably, especially for longer pulse durations.
© 2005 Elsevier Ltd. All rights reserved.

1. Introduction

Even if conventional lasers, diamond saws, and water jets are used commercially as a variety of cutting and machining utilities, none of them can achieve the precision of the femtosecond laser machine tool. In particular, industrial lasers that melt and boil material to remove it can cause substantial heat- and shock-induced damage to a circumference of the surrounding the cut, which ranges from deformations in the grain structure to global cracking. The damage may extend from a few micrometers to several millimeters from the cut, depending on material properties, laser pulse durations, and cooling mechanisms. Furthermore, even the slightest thermal stress or shock may create intolerable collateral damage, since very tiny structures only a few tens of micrometers in size, such as biological tissue or semiconductor devices, are extremely fragile. Contrary to these conventional ways, ultra-short pulse lasers represent a major advance in cutting technology and offer a great opportunity to machine materials with high precision that are difficult to achieve with conventional or nanosecond laser pulses.

It is known that laser-induced breakdowns are caused by three consequent mechanisms [1]: (i) the excitation of electrons in the conduction band by impact and multiphoton ionization (MPI), (ii) radiation-induced heating of the conduction-band electrons, and (iii) transfer of the plasma energy to the lattice. The key benefit of ultra-short femtosecond laser pulses lies in their ability to deposit energy in materials in a very short time interval. Heat diffusion is frozen during the interaction and the shocklike energy deposition leads to ablation for ultra-short pulses. This is because the pulse deposits its energy so quickly that it does not interact at all with the plume of vaporized material, which would distort and bend the incoming beam and produce a rough-edged cut. When ultra-short pulse lasers are used, the cut surfaces become very smooth and do not require subsequent cleanup, because only a very thin layer of

* Corresponding author. Tel.: +82 2 880 7117; fax: +82 2 883 0179.
E-mail address: jslee123@snu.ac.kr (J.S. Lee).

0017-9310/$ - see front matter © 2005 Elsevier Ltd. All rights reserved.
doi:10.1016/j.ijheatmasstransfer.2005.09.032

Nomenclature

D	diffusion coefficient, eV s^{-1}
E	electric field intensity, V m^{-1}
e	electron charge, C
F	normal distribution function for photo-generated electrons
F_{cr}	damage threshold fluence, J m^{-2}
f	electron distribution function, eV^{-1} m^{-3}, or the frequency of ac electric field, Hz
I	laser intensity, W m^{-2}
I_{cr}	critical laser intensity, W m^{-2}
I_0	maximum laser intensity, W m^{-2}
I_p	photon flux, m^{-2} s^{-1}
J	current, W m^{-5}
m^*	electron effective mass, kg
N_s	solid atom density, m^{-3}
n	electron number density, m^{-3}
n_c	plasma critical density, m^{-3}
P	multiphoton ionization, m^{-3} s
R	ionization source, eV^{-1} m^{-3} s^{-1}
R_J	Joule heating, eV s^{-1}
S	source, eV^{-1} m^{-3} s^{-1}
t	time, s
U_I	bandgap energy, eV
U_p	phonon energy, eV
V	effective electron heating, eV s^{-1}

Greek symbols

ε	electron energy, eV
$\hbar$	Planck constant, eV s
γ	energy loss rate, s^{-1}
λ	laser wavelength, m
ν_i	Keldysh impact ionization rate, s^{-1}
ν_m	momentum scattering rate, s^{-1}
σ	electrical conductivity, eV m^2 s^{-1} V^{-2}
$\sigma_{(K)}$	multiphoton ionization cross-section, m^{2K} s^{K-1}
τ	pulse duration, s
τ_m	moment scattering time, s
χ	Keldysh impact ionization rate constant, s^{-1}
ω	angular frequency of applied electric field, Hz

Subscripts

c	critical
el	electric field
imp	impact ionization
K	number of photons required to ionize the atom
la	laser
n	arbitrary number
p	photon
pi	multiphoton ionization

material is removed during each pulse irradiation of the laser. Although previous breakdown experiments [2–4] were recently extended to the sub-picosecond regime, the characteristics of the avalanche and the role of MPI have remained controversial even up to now.

Laser-induced damage can be regarded as one of the limiting factors of the transmission and deposition of laser energy on solids. The energy transfer mechanism of laser-induced damage is of great importance to the development of high-intensity lasers. Since several deterministic features for short-pulse damage have been discovered, many practical applications of femtosecond lasers have been developed in areas involving material removal with submicron precision, such as micromachining, ophthalmic surgery, electronics, data storage, and drug release. A large number of theoretical and experimental studies [2–6] have been conducted on laser-induced damage in dielectrics. Stuart et al. [3] reported extensive laser-induced damage threshold measurements on dielectric materials at wavelengths of 1053 and 526 nm for pulse durations ranging from 140 fs to 1 ns. They found that a gradual transition existed from the long-pulse, thermally dominated regime to an ablative regime dominated by collisional and multiphoton ionization (MPI), and plasma formation. In an investigation of interactions between laser-induced photons and energy carriers, Holway and Fradin [6] conducted simulations using the Fokker–Planck (F–P) equation. They took into consideration the nonpolar deformation potential effects for the electron–phonon interaction in defining the collision frequencies for momentum. Lenzner et al. [1] measured the damage threshold fluence and the ablation depth in dielectric materials for laser pulse durations ranging from 5 ps to 5 fs. They demonstrated that sub-10-fs laser pulses opened up a way to reversible nonperturbative nonlinear optics at intensities greater than 10^{14} W cm^{-2} slightly below damage threshold, and to nanometer-precision laser ablation in dielectric materials.

The ultimate goal of this article lies on examining the ultra-short pulse laser-induced damage characteristics in fused silica using the F–P equation. Extensive simulations are conducted to investigate the influence of laser pulse width on the transient behavior of electrons and the damage threshold fluence in SiO_2 dielectric material, and also to discuss the role of the impact ionization and the MPI in laser-induced damage. In addition, we have investigated the damage characteristics when both alternating current electric fields and ultra-short pulse lasers are applied simultaneously to the dielectric materials. This hybrid process is planned to confirm the possibility that the laser fluence required for breakdown would be lowered when a very high electric field is imposed on the material, compared to that without electric fields.

2. Analysis

Radiative energy of ultra-short pulse lasers ranging from pico to femtoseconds is absorbed much faster by the newly excited electrons than it is delivered from the electrons to the lattice. These electrons gain energy from the laser field until they have sufficient energy to collisionally ionize neighboring atoms thereby producing more free electrons. When laser is irradiated on materials, thermal effects should be considered in general. In ultra-short pulse laser applications, however, there would be no need to track the energy flow into the lattice to account for thermal and mechanical stresses, which is necessary for pulses longer than typically 50 ps [3]. As a matter of fact, it is possible to describe the plasma formation quantitatively by using the time dependence of the electron energy distribution function. Since the impact ionization rate depends highly on energy, the absorption rate of laser energy requires integrating over the electron energy distribution. When the electrons are strongly driven by intense laser pulses, the energy distribution can differ substantially from a Maxwellian. For material having a band gap energy that is much larger than the single photon energy, the heating and collisional ionization of conduction electrons can be described by the F–P equation, which is well known to be able to effectively describe the electron avalanche phenomena induced by an ultra-short pulse laser. For the estimation of electron distribution function $f(\varepsilon, t)$, the present work adopts the theoretical model of Stuart et al. [3] as follows:

$$\frac{\partial f(\varepsilon,t)}{\partial t} + \frac{\partial}{\partial \varepsilon}\left[V(\varepsilon,t)f(\varepsilon,t) - D(\varepsilon,t)\frac{\partial f(\varepsilon,t)}{\partial \varepsilon}\right] = \frac{\partial f(\varepsilon,t)}{\partial t} + \frac{\partial J(\varepsilon,t)}{\partial \varepsilon} = S(\varepsilon,t), \tag{1}$$

where ε is the electron kinetic energy. The number density of electrons with a kinetic energy between ε and $\varepsilon + d\varepsilon$ at time t is given by $f(\varepsilon, t)d\varepsilon$. The square bracket in Eq. (1) represents the change in the electron distribution due to Joule heating, inelastic scattering of phonons, and electron energy diffusion. In particular, $V(\varepsilon, t)$ consists of the Joule heating $R_J(\varepsilon, t)$ and the electron energy dissipation to phonon, $U_p\gamma(\varepsilon)$, given as,

$$V(\varepsilon,t) = R_J(\varepsilon,t) - U_p\gamma(\varepsilon), \tag{2}$$

where U_p is the characteristic phonon energy. $\gamma(\varepsilon)$ denotes the rate at which electron energy is transferred to the lattice, and it is determined from the experimental data of Sparks et al. [7]. The Joule heating term $R_J(\varepsilon, t)$ can be described by $\sigma(\varepsilon)E^2(t)/3$, where $E(t)$ is the electric field of the laser and $\sigma(\varepsilon) = e^2\tau_m(\varepsilon)/(m^*[1 + \omega^2\tau_m^2(\varepsilon)])$ is the ac electrical conductivity of a conduction-band electron of effective mass m^*. Here, $v_m(\varepsilon) = 1/\tau_m(\varepsilon)$ denotes the energy-dependent, electron–phonon transport (momentum) scattering rate, varying between 2 and 10 fs^{-1} from 1 to 10 eV for SiO_2 [8]. The diffusion coefficient $D(\varepsilon, t)$ [6] in Eq. (1) can be obtained by

$$D(\varepsilon,t) = \frac{2\sigma(\varepsilon)E^2(t)\varepsilon}{3} = 2\varepsilon R_J. \tag{3}$$

The last term in Eq. (1) denoting the total electron source is given by

$$S = R_{pi}(\varepsilon,t) + R_{imp}(\varepsilon,t), \tag{4}$$

where the first term on the right-hand side represents the generation of free electrons due to the MPI and second one due to the impact ionization. Generally, laser-induced breakdown is understood in terms of an electron avalanche in which conduction-band electrons, oscillating in response to the laser field, transfer energy by scattering from phonons [6]. If an electron can achieve the energy equal to the band gap, subsequent impact ionization promotes another valence electron into the conduction band. As shown in Fig. 1, electrons accelerated above ionization potential U_I, typically equal to the band gap energy of an electron, successively collide with neighboring atoms. An incident electron with kinetic energy, $\varepsilon_0 = 2\varepsilon + U_I$, produces two free electrons of energy, ε, and an ion of potential energy U_I in the final state. Impact ionization occurs at a rate described by the Keldysh impact formula [9], $v_i(\varepsilon) = 1.5(\varepsilon/U_I - 1)^2$, which is valid for incident electrons of energy smaller than 100 eV for fused silica [8]. The source term for impact ionization can be written as [6]

$$R_{imp}(\varepsilon,t) = -v_i(\varepsilon)f(\varepsilon,t) + 4v_i(2\varepsilon + U_I)f(2\varepsilon + U_I, t). \tag{5}$$

The last term on the right-hand side of Eq. (5) implies the electrons created by impact ionization. The term $v_i(\varepsilon)f(\varepsilon, t)$ represents the electrons that have been at the levels of their energies higher than the band gap energy before impact ionization. During the impact ionization process, these electrons transport their energies to other electrons in the valence band through the collisions with each other. Another contribution from the MPI, $R_{pi}(\varepsilon, t)$, can be modeled as $P(I)F(\varepsilon)$, where $P(I)$ is the MPI rate and $F(\varepsilon)$ is the normal distribution function for photo-generated electrons, so that $\int F(\varepsilon)\,d\varepsilon = 1$. The MPI rate can be simplified as [10]

$$P(I) = C_{(K)}I^K, \tag{6}$$

where $C_{(K)}$ denotes the proportionality coefficient for multiphoton ionization. The photon energy depends on

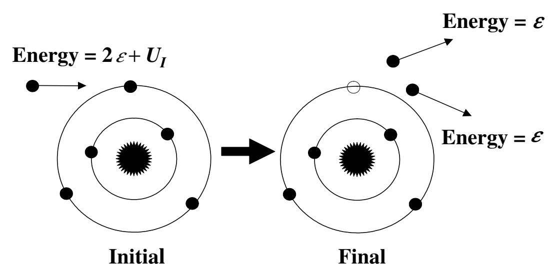

Fig. 1. Electron generation during impact ionization process.

its wavelength and the photoionization takes place when $Kh(c/\lambda)$ becomes larger than U_I. Here, K represents the minimum number of photons required to ionize the atom. For lasers of wavelength 526 nm, for instance, the number of photons should be larger than about 3.81 for overcoming the band gap energy. Four-photon absorption is therefore the relevant process for 526 nm light. From simply calculation, it can be easily indicated that more photons are needed for ionization as the wavelength becomes longer. The MPI rate for 526 nm becomes

$$P(I) = \sigma_{(4)}\left(\frac{I}{\hbar\omega}\right)^4 N_s, \tag{7}$$

where the quantity N_s is the solid atom density as listed in Table 1, and I is the intensity in TW/cm^2. For lack of information on $\sigma_{(K)}$ for fused silica, the present study uses the cross-section $\sigma_{(4)} = 2\times10^{-114}\ cm^8\ s^3$ which is measured for NaCl, as used by Stuart et al. [3] because other insulators have nearly the same value [11]. Since eight-photon absorption cross-section values are not available for 1053 nm light, the relationship $P(I) = 9.52\times10^{10}I^8$ obtained from the Keldysh expression [10] is used in the present simulation. This relationship is valid up to intensities on the order of $10^3\ TW/cm^2$ [10]. For extremely short intense pulses, tunneling ionization processes should be considered [3]. Since the maximum laser intensity considered in the present study is 10 TW/cm^2, the use of Keldysh expression may be appropriate. Calculated results are compared with experimental data of Stuart et al. [3]. In addition to the calculations for 1053 and 526 nm lights, the numerical simulation is conducted for $\lambda = 780$ nm and compared with the measurements of Lenzner et al. [1]. From the comparisons, evaluation of the Keldysh formula gives the proportionality coefficient $C_{(6)} = 6.0\times10^{8\pm0.9}\ cm^{-3}\ ps^{-1}\ (cm^2/TW)^6$ for multiphoton ionization on the basis of the assumption that the six-photon absorption process occurs at the wavelength 780 nm.

One-dimensional transient finite difference method is applied in the fully implicit manner to solve the F–P equation given in Eq. (1). As shown in Fig. 2, the irradiated pulse laser intensity is modeled by Gaussian with respect to time as follows:

$$I(t) = I_0 \exp\left(-4(\ln 2)\frac{t^2}{\tau^2}\right), \tag{8}$$

Table 1
Physical properties of SiO_2 used in this study

Parameter	Definition	Value
$\hbar\omega_p$	Phonon energy (eV)	0.0323 [7]
γ	Energy loss rate (ps^{-1})	200.0 [7]
m^*	Effective mass (kg)	9.109×10^{-31} [7]
e	Electron charge (C)	-1.602×10^{-19}
U_I	Bandgap energy (eV)	9.0 [3]
$\hbar$	Planck constant (J s)	1.054×10^{-34}
N_s	Solid atom density (cm^{-3})	1.401×10^{21} [11]
χ	Keldysh impact ionization rate (ps^{-1})	1500.0 [9]

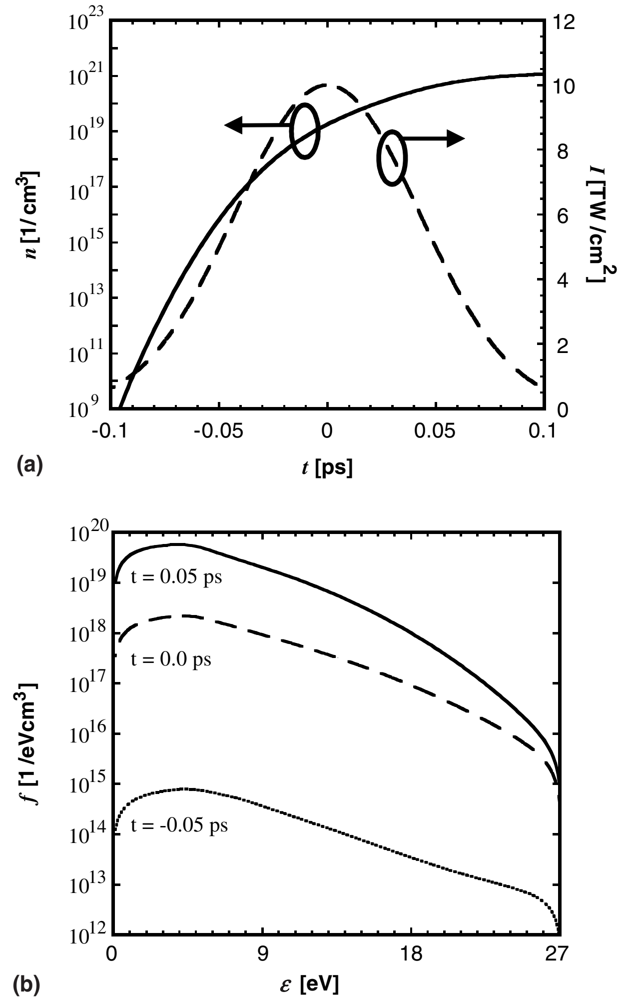

Fig. 2. (a) Electron number densities (solid line) and laser intensity (dashed line) with time and (b) electron distribution functions with electron energies at $t = -0.05$, 0.0, 0.05 ps for $\lambda = 1053$ nm and $I_0 = 10\ TW/cm^2$.

where τ denotes the pulse duration of irradiated laser beam and I_0 represents the maximum intensity of laser. Solving the F–P equation allows us to directly obtain the electron distribution function, $f(\varepsilon, t)$. The electron number density is calculated by

$$n = \int_0^\infty f(\varepsilon, t)\,d\varepsilon. \tag{9}$$

Initially, electron distribution functions are set to zero. Two boundary conditions should be applied in solving Eq. (1) and they are the current $J = 0$ at $\varepsilon = 0$ and the electron distribution function $f(\varepsilon, t) \to 0$ as $\varepsilon \to \infty$. The latter indicates that there is a bare possibility that the electrons would appear at the energy levels much higher than the conduction band. The present simulations are thus performed only in the range from $\varepsilon = 0$ to $\varepsilon = 3U_I$, where U_I is the band gap energy, 9 eV for SiO_2, on the basis of the assumption that the electron number distribution is negligible for $\varepsilon > 3U_I$ [3]. Damage threshold fluence can be pre-

dicted by postulating a threshold electron density associated with the onset of permanent damage. Formation of the critical density plasma has an important effect in the material processing with short pulse lasers. A plasma critical density of electrons, n_c, is defined as the density at which the energy density of conduction electrons equals the binding energy of the lattice. When $n > n_c$, laser-induced damage are assumed to occur. In the present study, the plasma critical density is assumed to be $n_c \approx 1.11 \times 10^{21}/\lambda^2\,\mathrm{cm}^{-3}$ from the available experimental results [9]. Damage threshold fluence can be written as follows:

$$F_{cr} = \int_{-\tau}^{+\tau} I(t)\,\mathrm{d}t = \int_{-\tau}^{+\tau} I_{cr} \exp\left(-4(\ln 2)\frac{t^2}{\tau^2}\right)\mathrm{d}t, \qquad (10)$$

where I_{cr} means the critical laser intensity at which laser-induced breakdown occurs. Generally, dielectrics are the materials with no free electrons and low thermal/electrical conductivity. Common material such as fused silica, sapphire, SiC, diamond, SiN, glass, heart tissue, and so on would fall under this category. Fused silica SiO_2 is used in the present calculation and its physical properties are listed in Table 1.

3. Results and discussion

Fig. 2(a) presents the predictions of electron number density and laser intensity with respect to time when $\lambda = 1053$ nm, the pulse duration is 0.1 ps, and the maximum laser intensity is 10 TW/cm^2. The electron number density continues to increase with time, but its rate of increase becomes gradually slower after laser intensity passes through its maximum value. Rapid growth of electron number density is caused by the substantial ionization owing to both impact ionization and MPI processes. The predictions of electron distribution functions at three different time locations are presented in Fig. 2(b) to show the variations of electron distribution with the energy level of electron. The electron distribution functions are found to increase with time beyond their maximum points. The number of electrons gradually decreases as the electron energy increases and most of electrons are distributed over the range from 0 to 9 eV that is equal to band gap energy. At $t = -0.05$ ps, for instance, the number of electrons occupying in the range of $0 < \varepsilon < 9$ eV is about 80% of the total number of electrons, whereas it is about 85% at $t = 0.05$ ps. The MPI process serves only for the production of seed electrons for the avalanche at the early stage of irradiation start, whereas the impact ionization process becomes more dominant in generating electrons than the MPI process as time goes on. If the impact ionization process becomes dominant, the successive collisions with a neighboring electron lead to the lost of much of electron energy that is above the band gap energy. Thus, most of the electrons participating in collisions are distributed below the band gap energy.

Fig. 3 represents the effects of the MPI and the avalanche (impact) ionization on the electron number density at different laser pulse widths. As the pulse width decreases, the electron number density increases obviously. The maximum electron density is about $10^{21}\,\mathrm{cm}^{-3}$ at $\tau = 0.01$ ps and the difference between the cases with and without considering the avalanche ionization effect is also very small. For shorter pulse widths, it can be concluded that the MPI alone generates sufficient electrons to cause damage effectively. In strong contrast with short pulse width, as the pulse width increases, the avalanche ionization process has a large effect on the increase of electron number density, especially after $t/\tau = 0$. For pulse width of 1.0 ps, the significant increase of electron number is especially observed over time when both MPI and avalanche ionizations are considered. Meanwhile, the reason why the avalanche ionization becomes dominant for longer pulse durations is that the avalanche ionization highly depends on the pulse duration. Contrary to the avalanche ionization, the MPI is mainly affected by the laser characteristics such as the laser wavelength and the pulse shape, in addition to laser intensity and duration. Thus, these basic mechanisms need to be clarified for fundamental understandings of the laser-induced damage characteristics in dielectrics.

Damage threshold fluence is defined as the critical laser energy per unit area at which the plasma is formed. Some investigators [1–4] reported that the damage threshold fluence scales approximately as $\tau^{1/2}$ in the long-pulse limit and then changes to the short-pulse limit near 20 ps. They observed a deviation from the $\tau^{1/2}$ scaling of breakdown threshold fluence and an increasingly deterministic character of breakdown for $\tau < 10$–20 ps as opposed to longer pulses. Fig. 4 implies that the calculated damage threshold fluences are in fairly good agreements with experimental observations of Stuart et al. [3] at $\lambda = 1053$ nm, whereas

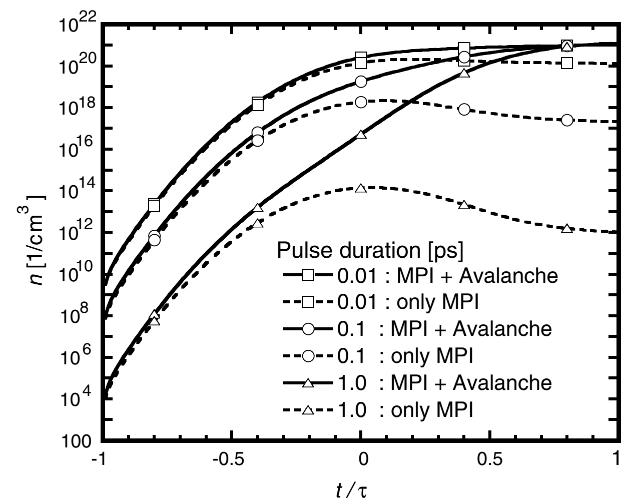

Fig. 3. Influence of multiphoton and avalanche ionizations on electron number density at different pulse durations for $\lambda = 1053$ nm and $I_0 = 10$ TW/cm^2.

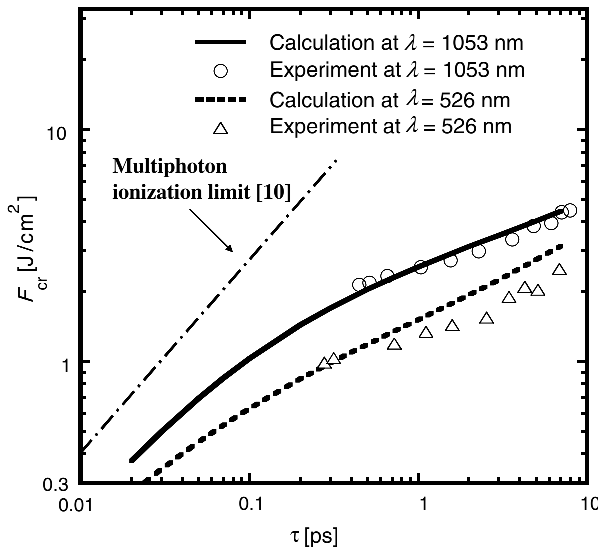

Fig. 4. Comparisons of the predictions of damage threshold fluences with experimental data of Stuart et al. [3] at $\lambda = 1053$ and 526 nm for various pulse durations.

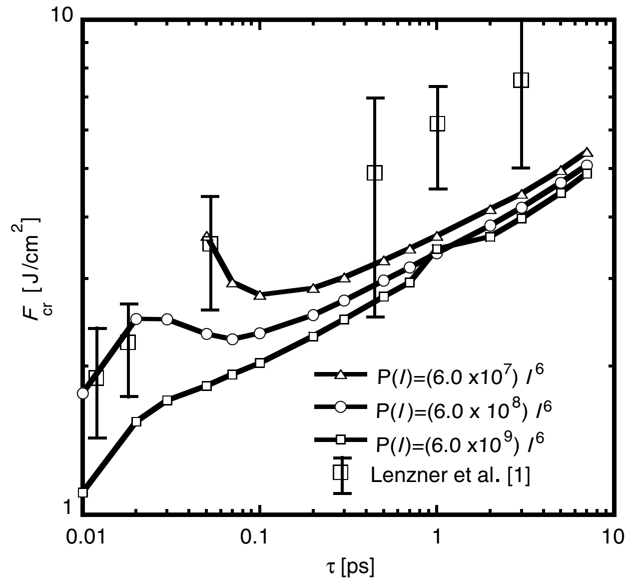

Fig. 5. Effects of multiphoton ionization rates on damage threshold fluences at $\lambda = 780$ nm for various pulse durations.

they are slightly over-predicted at $\lambda = 526$ nm. For pulses shorter than 10 ps, we should note that the damage fluence no longer follows the $\tau^{1/2}$ dependence and there exists the 'frozen region' of heat diffusion or the nonthermal region due to the nonequilibrium state between electrons and phonons, unlike thermal damage in long-pulse limit. It is also found in Fig. 4 that the damage fluence approaches to the multiphoton ionization limit as the pulse width decreases, as referred to by Perry et al. [10]. Generally, as the damage threshold fluence becomes smaller in machining any material, the efficiency of that laser machining system does higher. It is thus evident that the damage threshold fluence would be one of the most important factors in fabricating the material with high precision and saving cost. It is also noted in Fig. 4 that the damage threshold fluence decreases with reducing laser pulse width. As previously indicated in Fig. 3, it is because of the drastic growth of electron number density with decreasing laser pulse widths. Consequently, it suggests that laser fluence needed to cause damage is smaller for shorter pulses.

Above discussions are limited to the pulse range from 0.3 to several tens of picoseconds because the measured damage threshold fluences by Stuart et al. [3] are available for only pulses longer than 0.3 ps. Lenzner et al. [1] used 800 nm laser pulses ranging from 5 fs to 5 ps under 50 shots at 1 kHz to observe the laser damage nature in fused silica. The measurements reported by several researchers [2,5] have shown different dependence of damage threshold on pulse duration in the subpico-to-femto second regime. The present study uses the experimental data of Lenzner et al. [1] to investigate the laser-induced damage characteristics for a few femtosecond pulses. Fig. 5 compares the predicted damage threshold fluences using three different MPI rates, $P(I) = (6.0 \times 10^7)I^6$, $(6.0 \times 10^8)I^6$, and $(6.0 \times 10^9)I^6$ which are obtained from the results of Lenzner et al. [1]. Unlike the observations in Fig. 4, the damage threshold fluence becomes no longer lower than 1 J/cm^2, even at a 20-fs pulse. This is because the MPI rate at 780 nm is smaller than that at 1053 and 526 nm. Moreover, the damage threshold fluence rather increases for pulses shorter than nearly 100 fs. This feature is surprising at first because it is thought that the enhancement of MPI or other nonlinear effects reduce the damage threshold from the scaling rule for short pulses. Similar phenomena have been observed by Du et al. [2]. However, other measurements presented earlier have shown totally different characteristics from those of Du et al. [2] and the present calculations. Nevertheless, none of the theoretical and experimental investigators obviously explain this discrepancy in measurements and predictions. As discussed by Tien et al. [5], these discrepancies are perhaps thought to arise from different experimental conditions. Another point to note is that the damage threshold fluence decreases with increasing MPI rate. As indicated previously, the MPI becomes one of dominant channels in rapid increase of free electrons for ultra-short pulses that are typically shorter than several tens of femtosecond to sub-picosecond regimes. Therefore, when the pulse duration is very small, the decrease of MPI rate leads to suppress the increasing rate of free electrons and consequently much more laser fluence needs for the laser-induced damage in solids. Numerical predictions show satisfactory agreements with experimental data for both $(6.0 \times 10^7)I^6$ and $(6.0 \times 10^8)I^6$ cases. In spite of some discrepancies between predictions and measurements, it is thought that the numerical predictions are acceptable, taking into consideration the uncertainties of experimental data.

In what follows, the laser damage characteristics are discussed when both alternating current electric fields and ultra-short pulse lasers are simultaneously applied to the

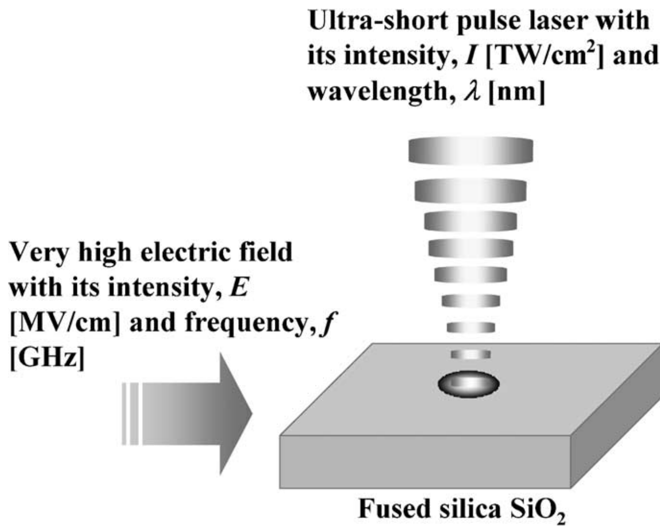

Fig. 6. Ultra-short pulse laser machining assisted by a high electric field.

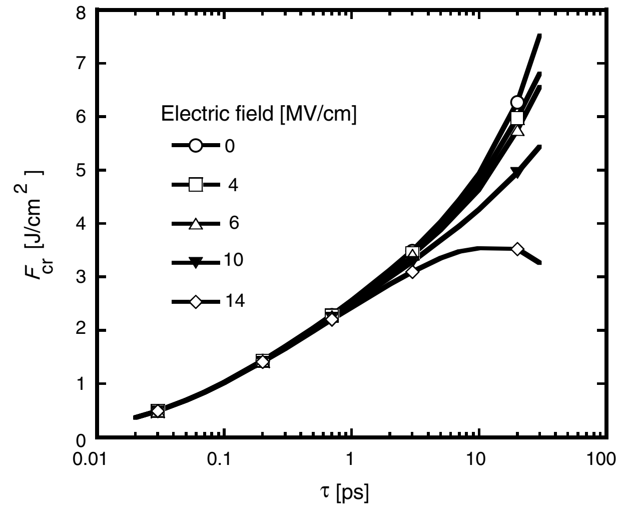

Fig. 7. Influence of applied electric fields on damage threshold fluence for different laser pulse durations at $\lambda = 1053$ nm.

dielectric materials as shown in Fig. 6. It is true that very high electric fields may allow the electron to reach an energy level sufficient to ionize, causing the impact ionization. As discussed earlier, the damage threshold fluence is closely associated with the efficiency of that laser machining system. This trial is thus planned to check whether the high electric fields can play a supplementary role in the generation of free electrons. In order to account for the electric field effects, Joule heating term $R_J(\varepsilon, t)$ in Eq. (2) is modified as,

$$R_J(\varepsilon,t) = R_{J_la}(\varepsilon,t) + R_{J_el}(\varepsilon,t) = \frac{\sigma_{la}(\varepsilon)E_{la}^2(t)}{3} + \frac{\sigma_{el}(\varepsilon)E_{el}^2(t)}{3}, \tag{11}$$

where the first term on the right-hand side is Joule heating term due to pulse laser irradiation and the second one due to the applied electric field. The electrical conductivity may be closely associated with the applied ac frequency. Since the frequency induced by the ultra-short laser pulse is much smaller than that of ac electric fields, however, the two terms appearing in Eq. (11) are assumed to be independent of each other, suggesting that the phase difference effects between the ac electric field and the laser pulse would be negligible. This assumption also comes from the fact that the electrical conductivity is dominated mainly by the momentum scattering rate of SiO_2, rather than the ac frequency. Fig. 7 shows the effects of applied electric fields at a fixed frequency of 1 GHz on the damage threshold fluence for different laser pulses at $\lambda = 1053$ nm. For $\tau > 3$ ps, the damage threshold fluence substantially decreases with increasing electric fields. It results from the fact that the amount of Joule heating due to the external electric field is of nearly the same order as that by the laser irradiation. This indicates that the excited electrons by external electric fields partly serve to the production of seed electrons for avalanche process. On the other hand, for pulses shorter than 1 ps, the electric field does not affect the changes of the damage threshold fluence at all. It means that the laser-induced damage becomes dominant more than the electric field-induced damage, because the magnitude of Joule heating by laser irradiation is much larger than that by the electric fields. Through further calculations, we could see that the electric field required to change the damage threshold fluence became about 10^2–10^3 MV/cm when $\tau < 1$ ps. This range of electric field is absolutely difficult to be reached from a practical point of view. Thus, it seems to be feasible for only sub-picosecond regimes that the electric fields can be used in accelerating the laser damage.

In addition, the frequency effects of electric ac fields upon laser damage feature are presented in Fig. 8. The relative changes of the damage threshold fluences are

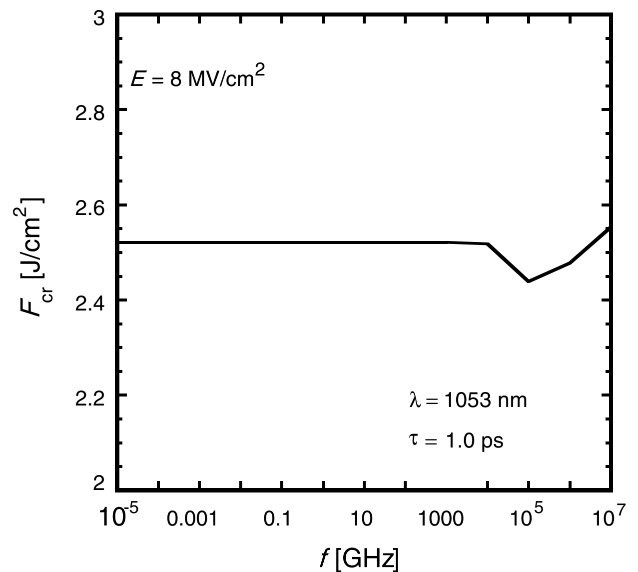

Fig. 8. Frequency effects of applied ac electric field on damage threshold fluence at $\lambda = 1053$ nm, $\tau = 1.0$ ps, and $E = 8$ MV/cm.

negligible with respect to field frequencies and furthermore, it may be impractical to apply those very high frequencies ranging from 10^4 to 10^7 GHz in order to reduce the threshold. These results are likely to result from the numerical simplicity because we assume in the present study that Joule heating due to pulse laser irradiation is independent of that due to applied electric ac field. Since there may exist other influences of applied electric fields in accelerating the electron generation process, however, further elaborate studies are needed to be performed in order to clarify a mechanism about the interactions between the applied electric ac field frequencies and the ionization of electrons.

4. Conclusions

The present article simulated the ultra-short pulse laser-induced damage on fused silica by using the Fokker–Planck equation. The following conclusions can be drawn.

Influence of laser pulses and wavelengths on laser damage threshold fluences was first investigated. As the laser pulse width decreases, the damage threshold intensity decreases and the MPI effect becomes more dominant than avalanche ionization effect. On the other hand, for longer pulses of laser, the impact ionization, i.e. avalanche ionization, becomes an important factor that contributes to the damage threshold of the dielectric material.

Unlike a few hundreds of femtosecond laser pulses, when the laser pulse duration is a few tens of femtoseconds, the damage threshold fluence does not decrease rather than 1 J/cm^2 or less. This limit seems to be persisted even with decreasing pulse width. However, the damage threshold may increase as the laser pulse decreases when the MPI effect is negligible.

Additionally, a hybrid scheme applying a high electric AC field simultaneously with the intense pulse laser was investigated to reduce the damage threshold intensity. This may reduce the damage threshold fluences considerably for relatively longer pulses, whereas it becomes ineffective for laser pulses shorter than 1.0 ps. The threshold fluences are found to be independent of AC frequencies of the applied electric fields except for very high frequencies.

Acknowledgement

The authors gratefully acknowledge financial support from the Micro Thermal System Research Center sponsored by the Korea Science and Engineering Foundation.

References

[1] M. Lenzner, J. Krüger, S. Sartania, Z. Cheng, Ch. Spielmann, G. Mourou, W. Kautek, F. Krausz, Femtosecond optical breakdown in dielectrics, Phys. Rev. Lett. 80 (18) (1998) 4076–4079.
[2] D. Du, X. Liu, G. Korn, J. Squier, G. Mourou, Laser-induced breakdown by impact ionization in SiO_2 with pulse widths from 7 ns to 150 fs, Appl. Phys. Lett. 64 (23) (1994) 3071–3073.
[3] B.C. Stuart, M.D. Feit, A.M. Rubenchik, B.W. Shore, M.D. Perry, Nanosecond-to-femtosecond laser-induced breakdown in dielectrics, Phys. Rev. B 53 (4) (1996) 1749–1761.
[4] F.H. Loesel, M.H. Niemz, J.F. Bille, T. Juhasz, Laser-induced optical breakdown on hard and soft tissues and its dependence on the pulse duration: experiment and model, IEEE J. Quantum Electron. 32 (10) (1996) 1717–1732.
[5] A. Tien, S. Backus, H. Kapteyn, M. Murnane, G. Mourou, Short-pulse laser damage in transparent materials as a function of pulse duration, Phys. Rev. Lett. 82 (19) (1999) 3883–3886.
[6] L.H. Holway Jr., D.W. Fradin, Electron avalanche breakdown by laser radiation in insulting crystals, J. Appl. Phys. 46 (1) (1975) 279–291.
[7] M. Sparks, D.L. Mills, R. Warren, T. Holstein, A.A. Maradudin, L.J. Sham, E. Loh Jr., D.F. King, Theory of electron-avalanche breakdown in solids, Phys. Rev. B 24 (6) (1981) 3519–3536.
[8] D. Arnold, F. Cartier, D.J. DiMaria, Acoustic-phonon runaway and impact ionization by hot electrons in silicon dioxide, Phys. Rev. B 45 (3) (1992) 1477–1480.
[9] C.V. Keldysh, Ionization in the field of a strong electromagnetic wave, Sov. Phys. JETP 20 (5) (1965) 1307–1314.
[10] M.D. Perry, B.C. Stuart, P.S. Banks, H.T. Nguyen, M.D. Feit, A.M. Rubenchik, J.A. Sefcik, Ultrashort-pulse laser machining, UCRL-ID-132159, Lawrence Livermore National Laboratory, University of California, 1998.
[11] S.C. Jones, P. Braunlich, R.T. Casper, X. Shen, P. Kelly, Recent progress on laser-induced modifications and intrinsic bulk damage of wide-gap optical materials, Opt. Eng. 28 (10) (1989) 1039–1068.